X-ray Diffraction Studies of Liquid Aluminum Alloy Oxidation

J.F. Moore,[1] K. Attenkofer,[1] W.F. Calaway,[1] J.N. Hryn,[1] B.V. King,[2] G.K. Krumdick,[1]
M.J. Pellin,[1] M.R. Savina,[1] G.B. Stephenson,[1] I.V. Veryovkin,[1] J. Zeh[3]
[1]Argonne National Laboratory, Argonne, IL, U.S.A.
[2]University of Newcastle, Newcastle, New South Wales, Australia
[3]Logan Aluminum, Russelville, KY, U.S.A.

Introduction

Aluminum oxidation during melting results in the loss of about 4% of the processed scrap in the aluminum industry, with a value of about $700 million dollars. In order to develop new ways of reducing this melt loss, we are studying the fundamental oxidation process of liquid aluminum alloys. In past studies that used mass gain methods, thickness growth rates on scales of only 1 μm or more were possible, followed by *ex situ* studies to identify phases that were present. Interesting but difficult-to-predict phenomena were observed, such as oxidation growth rates that depended on critical temperature and minor alloy compositions [1-3].

Our goal in this research was to develop a better understanding of what, if any, crystal structures are formed during the growth of oxide on liquid aluminum. Phase evolution in thin oxide films has been traditionally related to the growth mode (e.g., whether it is self-limiting, linear, or parabolic). In the system under study, the liquid state of the substrate must also be considered, since lattice matching is not strictly relevant and since diffusion is very fast relative to that in a solid system. Therefore, the wealth of knowledge that exists on oxide phases, growth kinetics, and even nucleation processes for solid intermetallics is not relevant to understanding oxide growth on liquid aluminum alloys.

Methods and Materials

X-ray diffraction (XRD) was performed on a number of molten aluminum alloy samples during their oxidation to track the phase evolution. Samples of aluminum alloys were taken from industrial melt furnaces and cut to an appropriate size by wire machining. Minor alloy constituents included Mg, Mn, and Fe. Our previous experiments had used a quartz cell with a heated block, which necessitated the use of high-energy photons (20 to 24 keV) to penetrate the quartz [4]. The new experiment used a cell fitted with large, water-cooled beryllium windows, which permitted the use of 8-keV x-rays. The lower x-ray energy has the advantage of providing higher-fluorescence cross sections for many of the elements under study, a higher critical angle, and higher diffraction angles (an aspect of the measurement that takes advantage of a large area detector). XRD patterns were taken with a fixed incidence angle by using the area detector; acquisition times were typically 10 seconds. Such rapid acquisition times were crucial for following the oxidation, since changes were often seen within minutes of when the oxidation conditions above the molten sample changed.

XRD patterns were measured on each sample before and after melting, after the surface was cleaned, during oxidation, just after solidification, and after cooling to room temperature. A temperature monitoring and control system was set up for remotely controlling the cell, gas, and sample temperatures. The greatest difficulty occurred in cleaning the sample of the initial oxide that formed on the sample during heating. A scraper was eventually used to remove the layer of dross (oxide and entrained metal) from the liquid, revealing a clean liquid metal surface. Oxide growth on the clean liquid surface represents growth not only on a large open pool but also on a freshly exposed liquid metal during flow, such as a sheet or an ingot of aluminum. In an industrial setting, these forms of alloy are commonly remelted, and it is possible that a large fraction of the oxide formed during remelting comes from growth on the flowing liquid surfaces.

The incident angle of the x-ray beam on the surface was set to 0.5° (above the critical angle). Although the meniscus that formed after the melting generated a range of angles of incidence, the geometry was such that the diffraction from deeply penetrating x-rays at larger angles of incidence was strongly attenuated. The sampling depth was estimated to be about 2 μm. Fluorescence measurements were also taken with a light-element-sensitive spectrometer mounted in a backscattering configuration to minimize the x-ray background. This provided compositional information to complement the XRD data.

Results and Discussion

The figure shows the result of one experiment on a 5182 alloy sample (about 5% Mg with other minor components) that was heated to 750°C (when it became molten) and oxidized with pure O_2. The diffraction rings from the images were integrated and are shown as individual curves in the figure. Each curve represents a progression of 10 minutes from the previous measurement and is offset for clarity. After about 1 hour, MgO formation was apparent. Growth progressed, and eventually macroscopic oxide islands formed. The liquid state of the substrate allowed the islands to move and

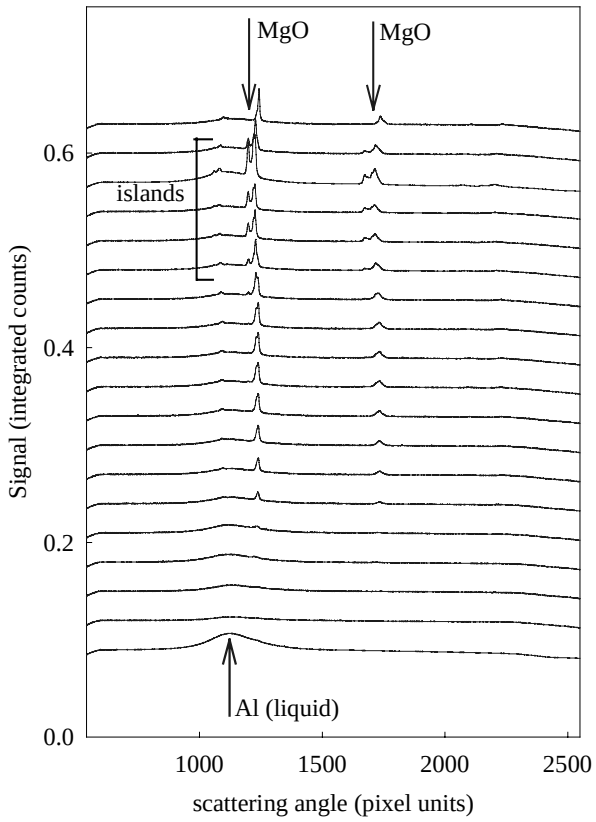

FIG. 1. Integrated radial XRD patterns, shown offset vertically with increasing time for clarity. The progression of a clean Al-Mg alloy (bottom) through an initial oxidation stage to the formation of large islands (top) is observed. The predominant oxide phase is identified as MgO for this alloy at 750°C under an oxygen atmosphere.

coalesce into a single structure (evidenced by the single peaks in the top curve). Fluorescence spectra confirmed the significant increase in Mg concentration near the surface in this experiment.

During oxidation, the Mg was drawn to the surface as a result of the chemical potential, forming an oxide such as MgO (cubic) or $MgAl_2O_4$ (spinel). These oxides can change composition during further oxide growth, depending on the other alloy components and the oxidizing conditions. As growth continued to the micron scale, the phases became well defined and less prone to further change, as the solid-state diffusion in the existing oxide layer became slow relative to the transport of the oxidizing gas (O_2 or H_2O) and cation transport from the bulk.

The gas composition was varied in the experiments, from pure O_2, to an Ar purge, to ambient air. The principal differences seen were in the growth rates of the oxide. In the 5182 alloy experiment described above, the rate was about 30 times faster in a pure O_2 environment than in the Ar purged environment. Interestingly, the presence of inclusions (as determined by sample origin and microscopy) had a more dramatic effect on the onset of oxidation and the ultimate oxide growth rate than did the composition of the alloy or the oxidizing atmosphere, although each of these factors had a significant influence. These experiments have yielded insight into the oxidation of molten aluminum alloys, and the results have suggested methods for reducing melt loss on an industrial scale.

Acknowledgments

Use of the APS was supported by the U.S. Department of Energy (DOE), Office of Science, Office of Basic Energy Sciences (BES), under Contract No. W-31-109-ENG-38. This work was supported by DOE BES and by Secat, Inc.

References

[1] C.N. Cochran, D.L. Belitskus, and D.L. Kinosz, Metall. Trans. B **8B**, 323-332 (1977).

[2] S. Impey, D.J. Stephenson, and J.R. Nicholls, in *Microscopy of Oxidation 2: Proceedings of the Second International Conference on the Microscopy of Oxidation Held at Selwyn College the University*, edited by M.J. Bennett and S.B. Newcomb (Maney Publishing, January 1994), pp. 338-346.

[3] F. Stucki, M. Erbudak, and G. Kostorz, Appl. Surf. Sci. **27**, 393-400 (1987).

[4] G.B. Stephenson et al., Mater. Res. Bull. **24**(1), 21 (January 1999).